JOURNAL OF MATERIALS SCIENCE **36** (2001) 1823–1832

# Zirconia infiltration toughening of Na-$\beta$-alumina

I. B. INWANG, I. J. McCOLM*,‡, A. WRONSKI§
*Department of ‡Industrial Technology and §Department of Mechanical Engineering, University of Bradford, Bradford BD7 1DP, UK*
*E-mail: I.J.McColm@bradford.ac.uk*

Disc and toroidal shaped samples of composites made from powders of Na-$\beta$-alumina and tin-stabilised tetragonal zirconia by conventional mixing and sintering processes have been used to establish data on the effect of the zirconia on the sintering efficiency, the mechanical strength, hardness and fracture toughness. These data have been compared to the results obtained when the $\beta$-alumina powder was first pre-sintered and then infiltrated with solutions of zirconium salts or suspensions of the tin-stabilised tetragonal zirconia. The results indicate that significant improvements to the mechanical properties can be made when the zirconia is introduced via an organometallic salt dissolved in an organic solvent. For the conventionally made samples the strength and toughness peak at 15 wt% zirconia addition. Sample densities in excess of 97% are achieved by pressurless sintering at temperatures up to 1600 °C. 

## 1. Introduction

The $\beta$-alumina family of compounds has the general formula $M_{1-x}Al_{11}O_{17+x/2}$. and a crystal structure in which the length of the *c*-axis depends both on the degree of non-stoichiometry, $x$, and on the particular charge balancing counter-ion, $M^{n+}$. For sodium-$\beta$-alumina the hexagonal unit cell parameters are $a = 0.560$ nm, $c = 2.253$ nm [1]. Ceramic membranes made from polymorphs in this family have resistivity values that are greatly affected by the crystallographic dimensions as well as by the microstructure and method of fabrication.

Cracking or fracture of ceramic membranes made from $\beta$-$Al_2O_3$ may be due to thermal or mechanical shock, the remedy for which has been sought in increasing the strength through pressure sintering methods. For fully dense, high strength, $\beta$-$Al_2O_3$ membranes of the type used in electrochemical cells, an electrochemically generated failure mechanism occurs: there is a critical current density which induces mechanical cracking of the membrane. It has been shown that the critical current density is directly proportional to the fourth power of the critical stress intensity factor, $K_{1C}$, [2]. Thus modest improvements in this mechanical property should result in longer membrane life and allow higher charging current densities to be used, which in turn would lead to reduced charging times.

The success in raising $K_{1C}$ values by the incorporation of metastable tetragonal $ZrO_2$ in various ceramic matrices [3, 4], led to such additions being made to $\beta$-$Al_2O_3$ [5, 6]. Addition of 15wt% $ZrO_2$ improved the mechanical properties, but unfortunately increased the ionic resistivity by forming an almost continuous, low conductivity phase along $\beta$-$Al_2O_3$ grain boundaries. This worsens an already bad situation arising from the highly anisotropic crystal structure of each grain, which means that not all grain-grain contacts in Na-$\beta$-$Al_2O_3$ contribute to conductivity. The crystal structure of sodium-$\beta$-$Al_2O_3$ confines the ionic mobility to *ab* planes perpendicular to the *c*-axis and conductivity arises from rapid migration of cations in loosely packed oxygen planes. These conducting planes are spaced at approximately 1.1 nm intervals between spinel blocks consisting of four close packed oxygen layers with $Al^{3+}$ ions in octahedral and tetrahedral sites. In contrast to the large conductivity in the open planes, the conductivity through the spinel blocks is very low [7]. Using conventional sintering methods, the grains often grow as flat platelets with their flat surfaces parallel to the conduction layers. When this occurs, only a small fraction of the microstructure provides access for $Na^+$ ions to be transported across the membrane. In a sodium-sulphur cell; for example it has been observed that resistivity decreases from 4.45-ohm cm to 2.84 ohm cm as the grain size is increased from 2 to 100 $\mu$m [8].

Current-generated mechanical failure is thought to occur from the extension of pre-existing surface cracks driven by stresses generated when $Na^+$ ions move to the sodium-filled tips of such cracks and are discharged. The discharge causes a flow of sodium from the crack which, because $Na^o$ is larger than $Na^+$, generates stress and cracks advance by a type of stress-corrosion mechanism.

Improvements to the life of $\beta$-$Al_2O_3$ membranes could therefore be sought by building-in crack arrest mechanisms and including sodium getter materials. Clearly the attempt to increase $K_{1C}$ for $\beta$-$Al_2O_3$ by the addition of zirconia as a crack arrest material can be successful, but the method leads to poor electrical properties. Here we report some experiments designed

* Author to whom all correspondence should be addressed.

TABLE I Critical stress intensity factor for Na-$\beta$-$Al_2O_3$

| Fabrication Route | Toughness method | $K_{1C}$ MN $m^{-3/2}$ | Reference |
|---|---|---|---|
| sintered | Indentation | 2.25 | 9 |
| sintered | SENB | 2.3-2.8 | 10 |
| hot pressed | Indentation | 2.24-2.35 | 10 |
| hot pressed | SENB | 3.6 | 11 |
| hot pressed | DCB | 2.7-3.7 | 11 |
| sintered | DCB | 3.2 | 12 |
| sintered | BNT | 2.7 | ) |
| sintered | BNT | 3.48 | ) 13 in 14 |
| sintered | BNT | 3.1 | ) |

Indentation = by direct crack length measurement.
DCB = Double Cantilever Beam.
SENB = Single-edge notched beam.
BNT = Bursting Notched Tubes.

to improve the mechanical properties by filling pores in $\beta$-$Al_2O_3$ pre-forms with metastable tetragonal zirconia and $\beta$-$Al_2O_3$. This technique would not interfere with the existing grain-grain contacts in the already pre-formed discs. The methods described here do not involve hot pressing, but do lead to samples with densities in excess of 95% theoretical and so such materials should have potential as electrodes.

The work focuses on raising the critical stress intensity factor value for $\beta$-$Al_2O_3$ and so for comparison Table I shows typical values for this property for $\beta$-$Al_2O_3$ made by two different methods and tested by four different techniques, against which any improvement can be judged. It seems, from the results in Table I, that where the indentation method is used to determine $K_{1C}$, the values obtained do not reflect the fabrication method. Furthermore the spread of values suggests that the indentation method, compared to other techniques, gives values at the low end of the range. However, it must be emphasised that the value obtained from the indentation technique reflects the equation used [15]. Despite this, the technique was used in this work in combination with the diametral compression strength test because both methods give data from small specimens. This was an advantage since all the $\beta$-$Al_2O_3$ and zirconia powders were made for the research in our laboratories and only small-scale methods were available, which limited the amounts of precursor material.

In essence, variation in the data as a result of uncertainties in the indentation models used was limited by using the techniques comparatively to assess the effect of zirconia content, and compare normal mixing methods to infiltration methods. The results suggest that considerable improvements to the mechanical properties can be made when zirconia infiltration via organometallic salts in organic solvents is used. This paper reports preparation methods and the results from the mechanical property tests.

## 2. Experimental

### 2.1. Preparation of starting powders

A solution of aluminium chloride in distilled water was prepared, filtered and then adjusted to pH 9–10 by adding ammonia solution. The resultant hydrous alumina gel was washed with water and acetone until the presence of $Cl^-$ ion was not detectable on addition of silver nitrate solution to the filtrate. The gel was dried at 120°C prior to calcination at 1000 °C. This gave an $\alpha$-$Al_2O_3$ powder of 20.6 nm average particle size. This powder was used, together with sodium carbonate, to make $\beta$-$Al_2O_3$ by three different routes:

(i) A slurry of the $\alpha$-$Al_2O_3$ in methanol was ultrasonically mixed with $Na_2CO_3$ powder calculated to give an 8.5% $Na_2O$ composition on firing. After drying at 80C the mixture was compacted into discs which were stacked in closed, re-crystallised alumina crucibles and heated at 1260 °C for two hours.

(ii) A combined suspension-solution freeze drying method where the $\alpha$-$Al_2O_3$ powder was suspended in $Na_2CO_3$ solution and then frozen rapidly in liquid nitrogen. By constant pumping, the frozen solid was eventually freeze-dried to an ultrafine powder, which was fired as in (i) above.

(iii) Solutions of $Al(NO_3)_3$ and $Na_2CO_3$ were mixed in the desired proportion to yield $\beta$-$Al_2O_3$ and sprayed through an atomiser into a glass tube surrounded by liquid. $N_2$. The frozen spray was continually pumped while the liquid $N_2$ was allowed to evaporate. Eventually, after several days pumping, an ultrafine powder, mixed on the atomic scale, was available for firing to $\beta$-$Al_2O_3$. Only limited work was done this way because of the time factor and the very small yields.

Tetragonal $ZrO_2$ and $Zr_{1-x}Sn_xO_2$ powders were made by precipitation of hydrous-gels from zirconium nitrate and stannous chloride solutions. The gels were filtered and thoroughly washed with distilled water before either freeze-drying or oven drying at 120 °C. Dried powders were heated to a temperature within the range 428–450 °C for one hour to convert them to the tetragonal polymorph.

### 2.2. Powder characterisation

(i) *Thermal analysis:* DTA-TG traces were obtained on a Stanton Redcroft Thermal Analyser, STA-780 using well-crystallised $\alpha$-$Al_2O_3$ as the standard and heating rates in the range 2–10 °C $min^{-1}$ in static air.

(ii) *X-ray powder diffraction*: Phase analyses were achieved using a Hägg-Guinier focusing camera, XDC-700 with Cu $k_{\alpha_1}$ radiation. Pure silicon, $a = 0.54308_8$ nm, was used to obtain the camera constant and to produce lines free from strain and particle-size broadening.

Line intensities were quantified using a Joyce-Loebel microdensitometer MK-111CS. Samples were analysed for their tet-$ZrO_2$ content using the method in ref [16], where the intensity of two lines, one from the tetragonal phase and the other from the monoclinic phase are compared.

For crystallite size measurements a Debye-Scherrer camera was used with mixtures of the powders with either silicon or $Y_5Si_3$ as reference. Average crystallite sizes were calculated from the width at half-peak-height using the Scherrer equation.

(iii) The sodium content of the powders and the sintered discs was found by first ion-exchanging the sodium for silver by heating at 220C for 24 hours with silver nitrate. The sodium in the silver nitrate was

determined by dissolving in de-ionised water and using a Baird A5100AA spectrophotometer in the emission mode. Previous calibration used Analar grade sodium nitrate solutions.

## 2.3. Disc fabrication

For each disc 2 g of powder was pressed uniaxially at pressures up to 140 MN $m^{-2}$, where they were held for 2 min, in a Beckmann-RIIC die of 13 mm diameter. At pressures above 132 MN $m^{-2}$ end-capping became a problem, and to reduce the number of discs spoiled by this delamination the following procedure was evolved: three weight per cent stearic acid was added to each batch suspended in methanol and agitated ultrasonically. After drying this mixture was pressed while evacuating the die.

By insertion of a central core, the die was modified to allow ring samples to be pressed from the same amount of powder at a pressure of 140 MN $m^{-2}$.

## 2.4. Sintering procedure

A vertical furnace heated by lanthanum chromite elements, Carbolite model B60/200, was used in conjunction with an Eurotherm 810 temperature controller and programmer. Pressed compacts were packed in a recrystallised alumina crucible and covered with loose $\beta$-$Al_2O_3$ powder of the same composition as the compacts. Oxygen was passed through the furnace whilst it was heated for 5.3 hr to reach 1620°C.

## 2.5. Composite preparation

Two methods were developed:

(i) *Vacuum infiltration*: The green discs were first pre-fired at 800 °C for 2–4 hours to be able to withstand the handling and infiltration conditions without disintegrating. The average density of each compact at this stage was 62%th. Five infiltrants were tried: $Al(NO_3)_3$ and $Zr(NO_3)_4$ solutions, a suspension of tetragonal $ZrO_2$, a suspension consisting of 20% $t$-$ZrO_2$ and 80% $\beta$-$Al_2O_3$, and a 30 mg $ml^{-1}$ solution of zirconium acetylacetonate in 80% acetone 20% water.

After each infiltration with the aluminium nitrate and/or zirconium nitrate solution the sample was heated to 400 °C after first drying at 100 °C to produce the oxides.

The discs were evacuated for 10 min. at a vacuum of $1.3 \times 10^{-3}$ Pa before the infiltrant solution or slurry was allowed into the reaction tube. Sonic agitation was applied for 10 min before the liquid was drained and a vacuum used to remove excess liquid. Each batch of discs was infiltrated in this way 10 times before oven drying and sintering.

(ii) *Wet mixing of $\beta$-$Al_2O_3$ and tin-doped tetragonal zirconia*: A co-gel of $ZrO_2$-$SnO_2$ was made from $Zr(NO_3)_4$ and $SnCl_2$ solution, washed, dried and calcined at 400 °C. The appropriate weight of this was mixed in methanol with $\beta$-$Al_2O_3$ in an ultrasonic bath. The dried, mixed powder was ball-milled and compacted for sintering.

After sintering each disc was characterised by determining the density from the mass and dimensions, as well as by a water displacement method.

Apparent porosity was determined by weighing in air ($W_D$), weighing while suspended in water ($W_B$) and weighing again in the air with water in the pores ($W_S$). The theoretical density was calculated from x-ray data.

X-ray characterisation was carried out on crushed material taken from fractured discs.

Fracture strength was determined at room temperature using the diametral compression test on the pellets, which were first polished on the faces to obtain two smooth parallel planes. A J.J. T20k tensile testing machine with a compression cage was employed using a 20 kN load cell and crosshead speed of 2 mm $min^{-1}$. Contoured anvils and a thin pad of cotton wool were used to obtain satisfactory load distribution. Any tests resulting in multiple fracture were rejected. Fracture strength was calculated from:

$$\sigma = \frac{2P}{\pi Dt} \tag{1}$$

where $P$ is the applied load, $D$ is the sample diameter and $t$ is the disc thickness. Where ring specimens were available, made to minimise the biaxial stress field associated with discs in this test, the alternative expression in Equation 2 was used:

$$\sigma_R = \frac{2Pk}{\pi Dt} \tag{2}$$

where $k$ is a stress concentration factor related to the relative hole radius $r$. The value of $k$ used was $6 + 38r^2$, as given by Hobbs [17].

Fracture toughness was measured by the indentation method. Samples were polished on silicon carbide papers down to 0.5 $\mu$m grade and finally with 0.1 $\mu$m Durmax alumina slurry. Indentations were made at loads in the range 0.98–1.96 N on a Leitz miniload microhardness tester and at higher loads from 2.45 to 29.4 N on a Vickers pyramid hardness tester. The load was applied for 15 s and the impression diagonals and crack lengths were measured immediately with the integral optical microscope. Where this was not possible, because of microstructural interference with the resolution, a photograph from the SEM investigation was used to make the measurements. Four indentations were made at each load from which mean values of diagonal and crack length were obtained. Indentations with obvious spaling were discarded and fresh ones made. If the indentation corners were displaced as a result of crack formation such measurements were not included to calculate the average. Toughness values were derived from the data by use of the two equations given in [15]:-

$$K_c = 0.0667\left(\frac{E}{H_v}\right)^{0.4} H_v a^{0.5}\left(\frac{c}{a}\right)^{-1.5} \tag{3}$$

for surface cracks where $0 = \frac{c}{a} > 2.5$ median or

$$K_c = 0.0181\left(\frac{E}{H_v}\right)^{0.4} H_v a^{0.5}\left(\frac{c}{a}\right)^{-0.5} \tag{4}$$

for Palmqvist cracks when $0.25 \leq \frac{c}{a} \leq 2/5$. Fig. 1 shows micrographs of indents made in infiltrated samples.

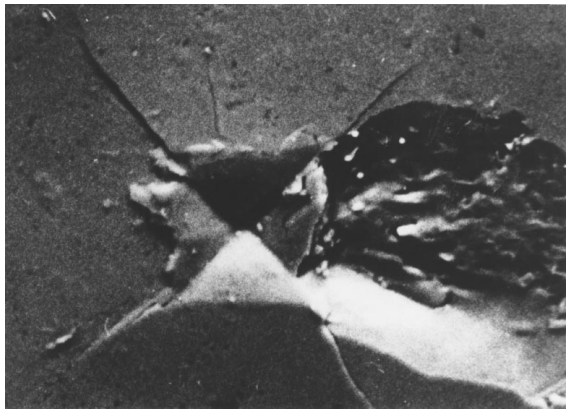

(A)

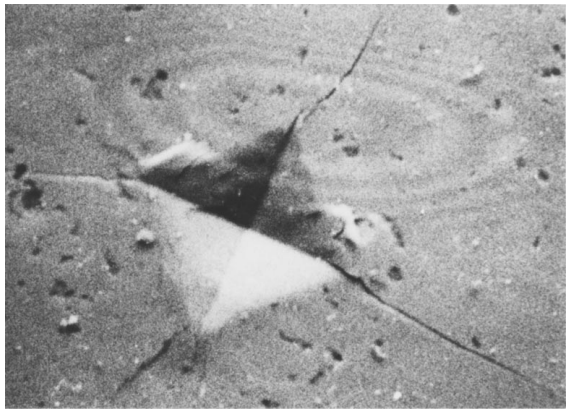

(B)

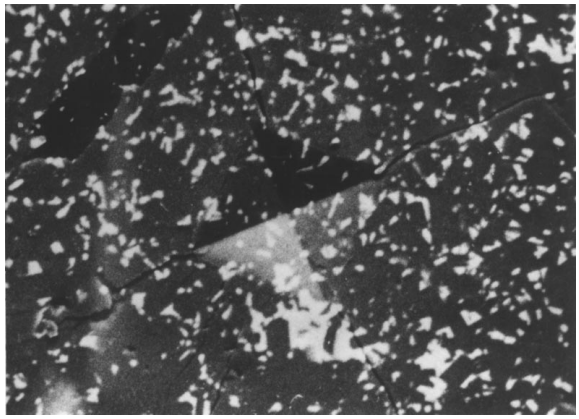

(C)

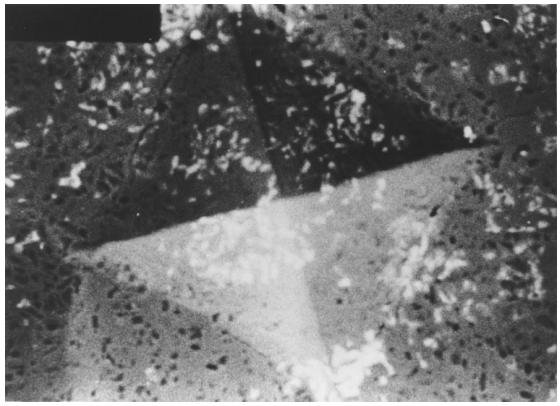

(D)

*Figure 1* SEM of $\beta$-$Al_2O_3$ showing indents and associated cracks: (A) Sample infiltrated with zirconia suspension; load 19.6 N, Mag. 510×. (B) Sample infiltrated with zirconia suspension; load 19.6 N; Mag. 680×. (C) Sample infiltrated with zirconium nitrate solution.; load 19.6 N; Mag. 350×. (D) Sample infiltrated with zirconium nitrate solution; load 4.9 N; Mag. 760×.

## 3. Results

The $\beta$-Alumina powders were not homogeneously single phase and the phase composition depended on the sodium content, as Tables II and III show. When the sodium content was equivalent to 5.24% $Na_2O$, unreacted $\alpha$-$Al_2O_3$ was present with the $\beta$-alumina phase which had a hexagonal cell with $a = 0.560_6$ nm, $c = 2.261$ nm. When the soda content was raised to 8.5%, $\beta$-alumina was present with large amounts of a $\beta''$-alumina which had hexagonal parameters $a = 0.599_8$ nm and $c = 3.40_7$ nm. The production of multiphase material is a well known problem [18–20]. Furthermore, because of the width of the diffraction lines and the large number of very faint ones, it is difficult to identify the $\beta$-phase formed or determine relative amounts by x-ray methods. The paper by Schmid [21] was useful in identifying the $\beta''$-alumina polymorph because he obtained diffraction patterns of pure $\beta$-$Al_2O_3$ and $\beta''$-$Al_2O_3$ and showed that the (014) and (017) planes are most characteristic for $\beta''$-alumina and $\beta$-$Al_2O_3$ respectively. It was decided, on the basis of the x-ray work, to use samples, which did not contain $\alpha$-$Al_2O_3$ for subsequent work, even though they may contain some $\beta''$-$Al_2O_3$.

To facilitate comparisons, the $\beta$-$Al_2O_3$ powders and the sintered compacts prepared by precipitation of $Al(OH)_3$, calcination, and wet mixing with $Na_2CO_3$, are called conventional-$\beta$-$Al_2O_3$ (CBA).

Both CBA powder and the freeze dried powder, after calcining, a particle size, around 20 nm. This probably arises from the fact that the freeze drying procedure involved $\alpha$-$Al_2O_3$ previously made by the gel precipitation technique. Both powders are highly agglomerated and show significant green density differences when compacted. The CBA powder gave higher green densities, but become end-capped at lower pressures. It was not possible to apply sufficient pressure on the discs to break up the agglomerates, as a graph of log

TABLE II X-ray powder data for 5.24% $Na_2O$ preparation

| Relative Intensity | hkl | $Sin^2\theta$ observed | $Sin^2\theta$ calculated * |
|---|---|---|---|
| VS | 002 | .0046 | $.0046_5$ |
| VS | 004 | .0183 | .0186 |
| VS | 012 | $\alpha$-$Al_2O_3$ | |
| S | 110 | .0749 | .0755 |
| M | 107 | .0816 | .0821 |
| M | 009 ) | .0941 | .0941 ) |
| | 114 ) | | .0941 ) |
| M | 200 ) | .1018 | .1007 ) |
| | 021 ) | | .1017 ) |
| M | 110 | .1046 | .1051 |
| M | 116 | .1174 | .1173 |
| M | 205 | .1293 | .1297 |
| VS | 113 | $\alpha$-$Al_2O_3$ | |
| M | 026 | .1427 | .1425 |
| W | 207 | .1569 | .1576 |
| S | 209 ) | .1962 | .1948 ) |
| | 0013 ) | | .1963 ) |
| VS | 217 ) | .2319 | .2331 ) |
| | 032 ) | | .2312 ) |
| M | 219 | .2692 | .2684 |
| VS | 036 | .3008 | .3008 |

* Calculated for an hexagonal cell $a = 0.5606$, $c = 2.26$ nm.

TABLE III X-ray powder data for 8.5% $Na_2O$ preparation

| Relative Intensity | hkl | $Sin^2\theta$ observed | $Sin^2\theta$ calculated * | Phase |
|---|---|---|---|---|
| VS | 002 | | | $\beta$ |
| | 003 | .0046 | 0046 | $\beta^{11}$ |
| VS | 006 | | 0184 | $\beta^{11}$ |
| | 004 | .0185 | 0186 | $\beta$ |
| M | 014 | .0332 | .0335 | $\beta^{11}$ |
| S | 110 | .0759 | .0754 | $\beta$ |
| | | | .0758 | $\beta^{11}$ |
| S | 017 | | | |
| | 114 | .0822 | .0821 | $\beta$ |
| S | 114 | | .0940 ) | $\beta$ |
| | 119 | | .0942 ) | $\beta^{11}$ |
| | 009 | .0941 | .0941 ) | $\beta$ |
| S | 020 | | .1007 ) | $\beta$ |
| | 021 | | .1017 ) | $\beta$ |
| | 020 | | .1010 ) | $\beta^{11}$ |
| | 117 | | .1008 ) | $\beta^{11}$ |
| | 021 | .1015 | .1015 ) | $\beta^{11}$ |
| S | 118 | | .1085 | $\beta^{11}$ |
| | 024 | .1089 | .1092 | $\beta^{11}$ |
| M | 119 | | .1172 | $\beta^{11}$ |
| | 116 | .1175 | .1173 | $\beta$ |
| S | 0114 | | .1255 | $\beta^{11}$ |
| | 207 | .1253 | .1260 | $\beta^{11}$ |
| S | 025 | .1296 | .1297 | $\beta$ |
| S | 1111 | .1361 | .1376 | $\beta^{11}$ |
| S | 026 | .1427 | .1424 | $\beta^{11}$ |
| | | | .1425 | $\beta$ |
| VS | 0210 | .1523 | .1521 | $\beta^{11}$ |
| S | 027 | .1581 | .1576 | $\beta$ |
| M | .0212 | .1741 | .1746 | $\beta^{11}$ |
| M | 216 | | .1952 | $\beta^{11}$ |
| | 029 | 1950 | .1948 | $\beta$ |

* calculated for $\beta$ $a = 0.560_6$ nm $c = 2.26$ nm;
$\beta^{11}$ $a = 0.599_8$ nm $c = 3.40_7$ nm.

(compacting pressure) against green density, indicated. Thus agglomerate strengths are in excess of 160 MPa. Table IV summarises the data.

## 3.1. Temperature and composition

The results in Fig. 2 show how the powder preparation method, composition and temperature affect the relative density of samples made from three of the powders. It is apparent that increased soda content has a marked effect, which supports the view that $\beta$-$Al_2O_3$ is generally difficult to densify without a transient liquid phase [22]. The 5.24% $Na_2O$ content samples could not be densified beyond 70%th. density, which is in agreement with an earlier finding by Hind and Robert [23]. The importance of oxygen in the sintering atmosphere is

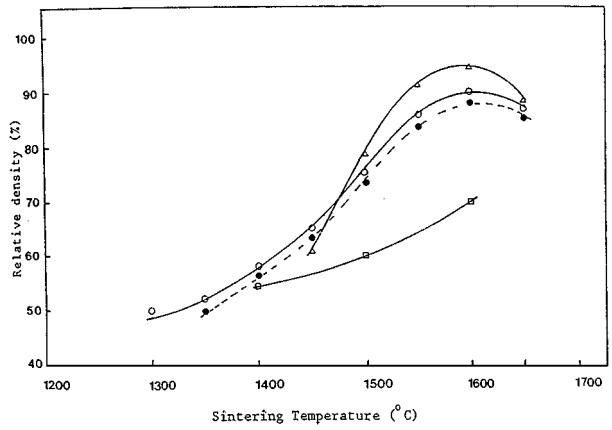


*Figure 2* Density-Sinter temperature relationship; ○-○-○ CBA 8.5% $Na_2O$; □-□-□ CBA 5.24% $Na_2O$; ●-●-●- CBA 8.5% $Na_2O$ sintered in air; △-△-△-suspension or solution formed $\beta$-$Al_2O_3$.

clear, with densities in excess of 95%th being achieved in flowing oxygen, hence this condition was used in all subsequent sintering tests done at an optimum temperature of 1600 °C. Fig. 2 clearly demonstrates the advantages of using the combined suspension-solution freeze dried powder to achieve the highest densities.

Analysis of sintered discs containing nominally 8.5% $Na_2O$ showed that in all cases sodium was lost and the final products contained 5.5% $Na_2O$, which is a small excess over the stoichiometric amount of 5.24%. This observation is in line with the x-ray diffraction analysis of the sintered samples which showed single phase $\beta$-$Al_2O_3$ with no lines unaccounted for.

## 3.2. Mechanical properties of sintered $\beta$-$Al_2O_3$ discs

A summary of data is given in Table V from which it can be seen that no consistent difference between samples made from CBA and the combined suspension-solution powders can be detected.

As expected, the mean fracture strength for ring specimens was significantly higher than that for the disc samples, which is a reflection of the difference in stress state and stressed volume. The mean fracture strength for the ring samples was 157 MN $m^{-2}$, which approaches the values around 180 MN $m^{-2}$ obtained by Binner and Stevens [9]. A study of isostatically pressed $\beta$-$Al_2O_3$ sintered at 1600°C for 1 hour reported a three-point bend strength of 114 MN $m^{-2}$ [24].

Weibull moduli are close to 14, regardless of powder type or specimen shape; this is good for a ceramic and

TABLE IV Comparative properties of the two types of $\beta$-$Al_2O_3$ powder

| Powder | Tap Density % Theoretical | Average Crystallite Size nm | Discs Pressed at 132 MPa | |
|---|---|---|---|---|
| | | | Density %th | DCS** MPa |
| CBA* (5.24% $Na_2O$) | 39.8 | 20.5 | 62 | 3.5 |
| CBA (8.5% $Na_2O$) | 40.0 | 20.6 | 62 | 3.5 |
| Suspension-Freeze Dried (8.5% $Na_2O$) | 36.0 | 20 | 59 | 3.2 |

* CBA refers to conventionally prepared $\beta$-alumina (see text).
** DCS is the diametral compression strength.

TABLE V Bulk mechanical properties of sintered $\beta$-$Al_2O_3$

| Sample Geometry | CBA Disc | CBA Ring | Combined suspension solution Disc |
|---|---|---|---|
| Strength $MNm^{-2}$ | 102 | 165 | 114 |
| | 107 | 156 | 106 |
| | 111 | 168 | 109 |
| | 99 | 157 | 96 |
| | 107 | 162 | 106 |
| | 105 | 140 | 104 |
| | 120 | — | — |
| | 113 | — | — |
| | 108 | — | — |
| Average $MNm^{-2}$ | 108 | 157 | 104 |
| Standard deviation. | 6 | 9 | 6 |
| Weibull modulus | 13.6 | 13.8 | 13 |
| Fracture toughness $MNm^{-3/2}$ | $3.4 \pm 0.1$ | | $3.2 \pm 0.1$ |
| Hardness $GNm^{-2}$ | $10.3 \pm 0.3$ | | $10.1 \pm 0.3$ |
| Density %th. | 93 | 95 | 93 |
| Apparent porosity % | 3.0 | 2.0 | 2.4 |
| True porosity % | 6.8 | 4.0 | 5.3 |

reflects favourably on the reproducibility of the powders and the processing method.

Fracture toughness values around 3.3 MN $m^{-3/2}$ lie in the range shown in Table I. They are larger than the 2.5 MN $m^{-3/2}$, also obtained by an indentation method, but using an alternative analysis [9].

In general these data show that either type of precursor powder could be used to fabricate the $\beta$-$Al_2O_3$ discs for the zirconia infiltration experiments and therefore the conventional powder was mostly used to make the composites. All were sintered at 1600C in oxygen enriched atmospheres.

### 3.3. $\beta$-$Al_2O_3$ - Zirconia composites made by conventional wet mixing

A 7 wt% $SnO_2$ - $ZrO_2$ powder, mean crystallite size 14.5 nm, was wet-mixed with the $\beta$-$Al_2O_3$ powder to give samples ranging from 5 to 25 wt% $ZrO_2$. Post sinter-density and other properties are gathered in Table VI and the relationship between strength, toughness, hardness and zirconia content is displayed graphically as Fig. 3. Increases in strength and toughness peak at 15 wt% $ZrO_2$, which is also the composition at which a retained tetragonal structure for the $ZrO_2$ is a maximum at 57%.

Sintering in the presence of zirconia leads to improved density and slightly decreased porosity. Fig. 4

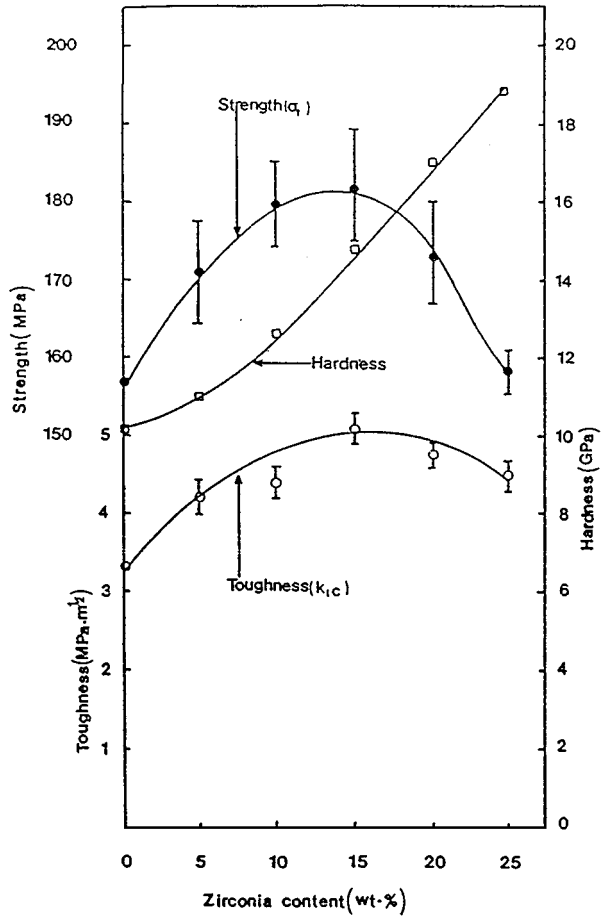


*Figure 3* The effect of zirconia additions on the strength, hardness and toughness of sintered CBA-$\beta$-$Al_2O_3$.

is an electron micrograph of an etched, fracture surface of a 5 wt% $ZrO_2$ sample in which there is evidence of exaggerated grain growth as well as of a fine dispersion of white $ZrO_2$ particles and isolated porosity. A significant number of all fracture origins occurred from large isolated internal pores, approximately 250 $\mu$m in size. Results in Table VII show that the calculated flaw size obtained from Equation 5:-

$$c = (K_{1c}/2\sigma_f)^2 \quad (5)$$

is in general agreement with the size of the suspected fracture initiating pore.

The size of the large grains identified in Fig. 4 is only in the 20–80 $\mu$m range, which suggests that they were not implicated in fracture initiation. The large pores

TABLE VI Properties of conventionally wet-mixed and sintered $\beta$-$Al_2O_3$-$ZrO_2$ composites

| $ZrO_2$ content wt.% | Density %th. | True porosity % | Apparent porosity % | Tetragonal $ZrO_2$ % | Strength MN $m^{-2}$ | Toughness MN $m^{-3/2}$ | Hardness GN $m^{-2}$ |
|---|---|---|---|---|---|---|---|
| 0 | 95 | 4.0 | 2.0 | — | $157.1 \pm 9$ | 3.3 | 10.2 |
| 5 | 95 | 4.9 | 2.0 | 10 | $171.1 \pm 6$ | 4.2 | 11.0 |
| 10 | 95 | 4.6 | 1.6 | 13 | $178.0 \pm 5$ | 4.4 | 12.6 |
| 15 | 96 | 4.0 | 1.0 | 57 | $181.4 \pm 8$ | 5.1 | 15.7 |
| 20 | 97 | 2.8 | 0.6 | 30 | $174.0 \pm 6$ | 4.6 | 17.0 |
| 25 | 97 | 1.2 | 0.5 | 38 | $158.0 \pm 3$ | 4.5 | 18.8 |

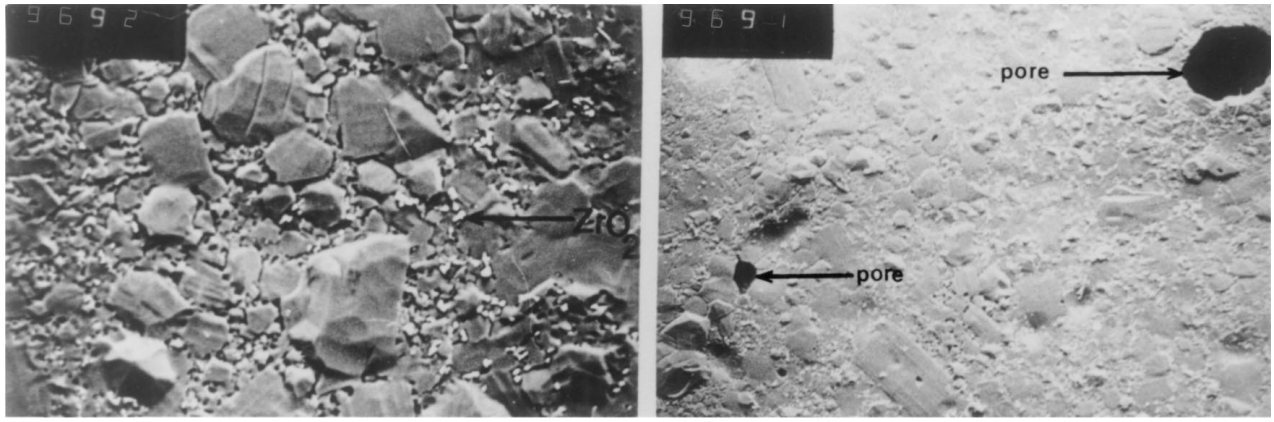


*Figure 4* SEM of CBA-$\beta$-$Al_2O_3$ + 5wt% $ZrO_2$ sintered at 1620C.

TABLE VII Calculated critical flaw sizes

| Sample | Fracture strength MN $m^{-2}$ | Fracture toughness MN $m^{-3/2}$ | Critical flaw size $\mu$m |
|---|---|---|---|
| CBA | | | |
| disc | 108 | 3.4 | 248 |
| ring | 157 | 3.4 | 117 |
| Combined suspension-solution disc | 104 | 3.2 | 237 |
| 5% zirconia | 171 | 4.2 | 151 |
| 15% zirconia | 181 | 5.1 | 198 |
| 20% zirconia | 174 | 4.6 | 175 |
| 25% zirconia | 158 | 4.5 | 203 |

TABLE VIII Weibull moduli for composites of CBA and $ZrO_2$ made by wet mixing

| Zirconia content % | *m* value |
|---|---|
| 0 | 14 |
| 5 | 14 |
| 10 | 13 |
| 15 | 11 |
| 20 | 12 |
| 25 | 17 |

are thought to arise in the pressing process as voids between agglomerates that sintering exaggerates and does not remove.

Although zirconia is not particularly well distributed by this purely mechanical mixing method, it acts in such a way as to limit the $\beta$-$Al_2O_3$ grain size during firing. For example the pure $\beta$-$Al_2O_3$ has $\sim$80 $\mu$m grains, while for 5% $ZrO_2$ this decreases to $\sim$60 $\mu$m and the 15% $ZrO_2$ samples have an average grain sizes of 21 $\mu$m.

Weibull plots for the strength data give the *m* values in Table VIII, which show that all the samples give values, which lie between 11 and 17. These are comparatively high for ceramics where values generally lie between 5 and 20 [25].

### 3.4. Composites made by the infiltration method

The first experiments involved $\beta$-$Al_2O_3$ compacts sintered to low density, approx. 70% theoretical. These were easy to handle and were infiltrated, after evacuation, with a mixed solution (7 : 1) $Al(NO_3)_3 : Na_2CO_3$. After drying the discs were heated to 1260 °C for 2 hours. This cycle was repeated ten times after which the density had increased to 75%th. From this it was concluded that much higher starting densities were needed when pore filling with $ZrO_2$ was to be tried. Accordingly a series of experiments was conducted where the starting density of the $\beta$-$Al_2O_3$ compacts varied from 63% to 90%th and the infiltrant was $Zr(NO_3)_4$ solution. Specimens were heated to 400C to produce $ZrO_2$ after each infiltration; measurements showed that inter-connected pore filling stops after 7 cycles, probably because the outer regions of the compact become blocked. This suggestion is partly supported by Fig. 5, where the zirconia shows as bright areas in a back scattered electron diffraction picture of the fracture surface of a disc. Clearly the zirconia from $Zr(NO_3)_4$ infiltration is not evenly distributed and is concentrated in the outer regions. This was confirmed on an EDX scan across the surface where area $A'$ had 4 times the zirconia concentration. Gross defects present in the pre-sinter are very obvious, which explains why only modest increases in strength are recorded after infiltration.

Table IX contains data for mechanical property values when a variety of infiltrant solutions were used. It can be seen that exceptional improvements are made when acetone-water zirconium acetylacetonate solutions are employed. When expressed as percentages the zirconium acetylacetonate solutions effected 20%, 67% and 37% improvements in strength, fracture toughness and hardness respectively. These samples had 42% retained tetragonal zirconia.

Densities around 96%th could be achieved for all types of infiltration, but the presence of residual pores some 150–230 $\mu$m in size provided obvious fracture initiation sites. These are approximately the same size as those causing failure in the wet-mixed-sinter samples and so limit the advantages of the infiltration method.

## 4. Discussion

The wet-mix method of composite preparation, where agglomerated tetragonal $ZrO_2$-7% $SnO_2$ powders of 14.5 nm mean diameter were added to pre-formed $\beta$-$Al_2O_3$ prior to uniaxial pressing and pressureless

TABLE IX Mechanical properties of $\beta$-alumina after various zirconia treatments

| Preparation | $ZrO_2$ wt% | Strength MN $m^{-2}$ | $K_{1c}$ MN $m^{-3/2}$ | strength increase % | toughness increase % |
|---|---|---|---|---|---|
| Uniaxial pressing | 0 | 108 (d) | 3.3 | — | — |
| sintered at 1620C | | 157 (R) | | | |
| Wet mixing and | 5* | 171.1(R) | 4.2 | 9 | 27 |
| uniaxial dry pressing | 10* | 178 (R) | 4.4 | 13 | 33 |
| sintered at 1620C | 15* | 181.4 (R) | 5.1 | 16 | 55 |
| | 20* | 174 (R) | 4.6 | 11 | 39 |
| | 25* | 158 (R) | 4.5 | 1 | 36 |
| Uniaxial dry pressing | 14.6 | 163 (R) | 3.9 | 4 | 18 |
| sintered at 1620C and then infiltrated with (i) $Zr(NO_3)_4$ solution | | | | | |
| (ii) t-$ZrO_2$ suspension | 14.6 | 170 (R) | 4.2 | 8 | 27 |
| both re-heated to 400C | | 117 (d) | 4.2 | 8 | 27 |
| Uniaxial dry pressing | 14 | 168 (R) | 3.9 | 7 | 18 |
| pre-sintered at 800C vacuum infiltrated with (i) $Zr(NO_3)_4$ solution | | | | | |
| (ii) t-$ZrO_2$ suspension | — | 177 (R) | 4.2 | 13 | 27 |
| | | 125 (d) | 4.0 | 16 | 21 |
| (iii) $\beta$-$Al_2O_3$ + t-$ZrO_2$ suspension | — | 160 (R) | 3.6 | 2 | 9 |
| (iv) zirconium acetylacetonate-acetone - water solution. All sintered at 1620C | — | 188 (R) | 5.5 | 20 | 67 |

d = disc and R = ring specimens. * The zirconia was stabilised with 7 vol% $SnO_2$.

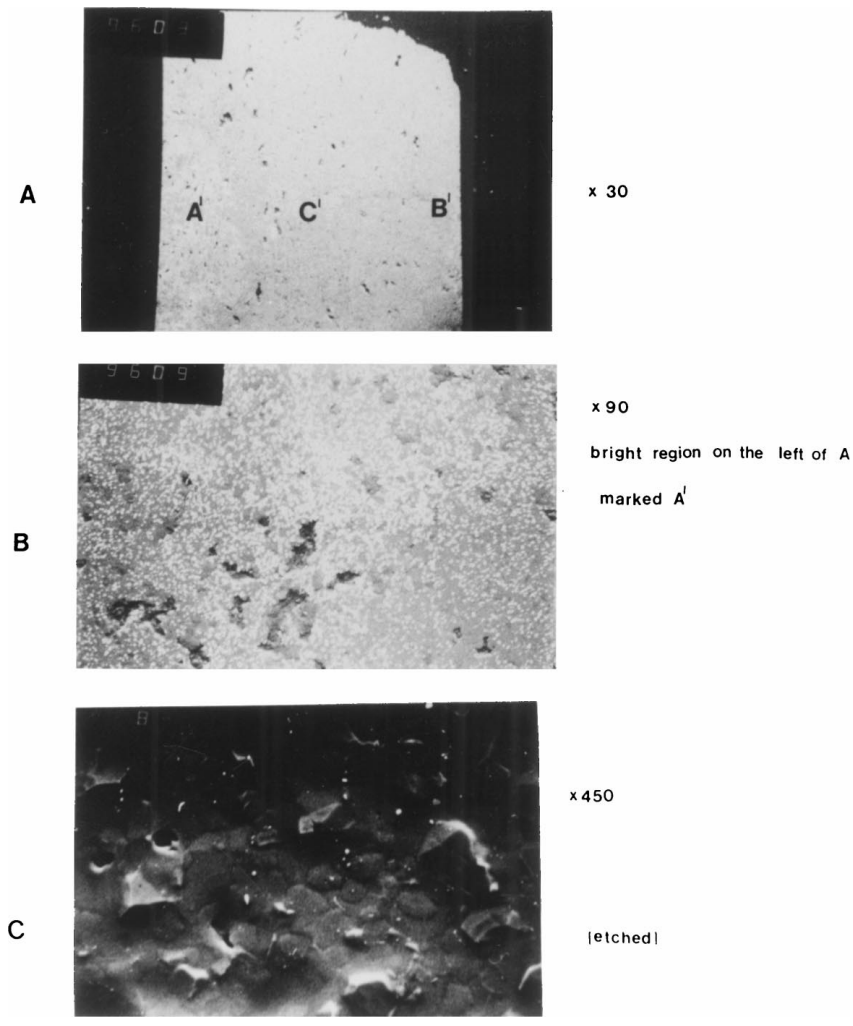


*Figure 5* Fracture surface of (A) $Zr(NO_3)_4$ infiltrated Na-$\beta$-$Al_2O_3$; (B) is region *A′* at higher magnification; (C) etched surface of a fractured disc after zirconyl acetylacetonate infiltration.

TABLE X Some literature results for mechanical properties of toughened $\beta$-alumina

| Sample Preparation | Zirconia wt.% | Values | | Increase | | Ref. |
|---|---|---|---|---|---|---|
| | | Strength MN $m^{-2}$ | Toughness MN $m^{-3/2}$ | Strength % | Toughness % | |
| Mechanical mixing, die pressing. | 15 | 262 | 2.82 | 10 | 15 | 9 |
| Sintered at 1620C | | (238) | (2.25) | | | |
| Wet mixing. Cold isostatic pressing. Sintered at 1600C | 24 | 350 | 4.51 | 60 | 100 | 28 |
| Wet mixing. Cold isostatic pressing. | 15 | 310 | 8 | 80 | 220 | 6 |
| Sintered at 1600C | (unstabilised) | (172) | (2.5) | | | |
| Slip cast. Sintered at 1535C | 24 | 354 | 5 | 141 | 67 | 27 |
| | | (147) | (3) | | | |

( ) values are for $\beta$-$Al_2O_3$ without added zirconia.

sintering, produced discs that showed improvements in mechanical properties over those measured for $\beta$-$Al_2O_3$. An optimum addition of 15 wt% $ZrO_2/SnO_2$ produced 55% and 16% increases in toughness and strength respectively, when 57% of the $ZrO_2$ was retained in the tetragonal form after sintering.

Table IX shows that no significant improvement was effected when infiltration routes were used except when the infiltrant was zirconium (iv)-acetylacetonate. However improvements to green state forming, so that defects as large as 150–200 $\mu$m are not formed, will be necessary to gain the ultimate improvements that can be achieved when tetragonal zirconia is infiltrated via the acetylacetonate method.

The improvements in the properties of zirconia toughened material, compared to pure $\beta$-$Al_2O_3$, reported here, are in keeping with the results from other workers who have used a pressureless sintering route [6, 9, 26, 27]. Data from these earlier reports are collected in Table X.

The comparisons of toughness values is not so simple, because the Evans and Charles method [29] was used by [6, 26, 27), the Anstis method [13] by [9], while here the method of Niihara [30, 31] was used. All these methods are load dependent and can lead to a 100% variation in toughness. Notwithstanding all this, with the exception of the 8 MN $m^{-3/2}$ value for $K_{1c}$ reported by Viswanathan *et al*. [6], the results obtained here are in the general range of results already reported. Additions of zirconia do inevitably improve toughness with the 5.5 MN $m^{-3/2}$ value for zirconium acetylacetonate infiltration samples being at the high end of improvements to the starting material. This improvement was achieved when only 42% of the zirconia was retained in the tetragonal form, which suggests that the mechanism contributing most to the improved toughness is probably one of crack deflection rather than phase transformation.

The maximum improvement in both mechanical properties from the conventional mixing method was achieved with a 15% addition in all cases. It was observed that additions beyond 15% resulted in increased porosity after sintering, with subsequent degradation in strength and toughness. The almost doubling of the fracture toughness by infiltration of zirconium acetylacetonate into sintered porous $\beta$-$Al_2O_3$ pre-forms should lead to significant increases in membrane life in Na-sulphur cells where $\beta$-$Al_2O_3$ membranes are used. This should be achieved without impairing ionic conductivity because the added zirconia is in pre-existing pores and will not hinder already formed $\beta$-$Al_2O_3$-$\beta$-$Al_2O_3$ contacts.

## References


1. C. R. PETERS, M. BETTMAN, J. W. MOORE and M. D. GLICK, *Acta Cryst. B* **27** (1971) 1826.
2. A. V. VIRKAR, *J. Mater. Sci*. **16** (1981) 1142.
3. N. CLAUSSEN, *J. Amer. Ceram. Soc*. **61** (1978) 85.
4. D. J. GREEN, *ibid*. **65** (1982) 610.
5. J. R. G. EVANS, R. STEVENS and S. R. TAN, *J. Mater. Sci*. **19** (1984) 4068.
6. L. VISWANATHAN, Y. IKUMA and A. V. VIRKAR, *ibid*. **18** (1983) 109.
7. R. W. POWERS, *J. Electrochem. Soc*. **122** (1975) 490.
8. G. E. YOUNGBLOOD, G. R. MILLER and R. S. GORDON, *J. Amer. Ceram. Soc.* **61** (1978) 86.
9. J. G. P. BINNER and R. STEVENS, *J. Mater. Sci*. **20** (1985) 3119.
10. A. V. VIRKAR, G. J. TENNENHOUSE and R. S. GORDON, *J. Amer. Ceram. Soc*. **57** (1974) 508.
11. A. V. VIRKAR and R. S. GORDON, *ibid*. **60** (1977) 58.
12. G. J. MAY, *J. Power Sources* **3** (1978) 1.
13. G. R. ANSTIS, P. CHANTIKUL, B. R. LAWN and D. B. MARSHALL, *J. Amer. Ceram. Soc*. **64** (1981) 533.
14. G. J. MAY and S. R. TAN, *Electrochimo Acta* **24** (1979) 755.
15. I. J. McCOLM, "Ceramic Hardness" (Plenum Press, New York, 1990) p. 145.
16. P. A. EVANS, R. STEVENS and J. G. P. BINNER, *Trans. J. Brit. Ceram. Soc*. **83** (1984) 39.
17. D. W. HOBBS, *Int. J. Rock Mech. Min. Sci.* **1** (1964) 385.
18. J. D. HODGE, *Ceram. Bull*. **62** (1983) 244.
19. J. RAABE, A. SZYMANSKI, W. WLOSINSKI and W. TOMASSI, *Electrochim. Acta* **24** (1979) 31.
20. D. J. M. BEVAN, B. HUDSON and P. T. MOSELEY, *Mater. Res. Bull*. **9** (1974) 1073.
21. C. SCHMID, *J. Mater. Sci. Lett*. **5** (1986) 263.
22. U. CHOWDHRY and R. M. CANNON, *Mater. Sci. Res*. **11** (1978) 443.
23. D. HIND and E. W. ROBERTS, *Trans. and J. Brit. Ceram. Soc*. **80** (1981) 219.
24. T. L. FRANCIS, F. E. PHELPS and G. MACZURA, *Amer. Ceram. Bull*. **50** (1971) 615.
25. R. W. DAVIDGE, "Mechanical Behaviour of Ceramics" (Cambridge University Press, 1980) p. 37.

26. F. F. LANGE, B. I. DAVIS and D. O. RALEIGH, *Comm. Amer. Ceram. Soc*. **63** (1983) C-50.
27. D. J. GREEN and M. G. METCALF, *Amer. Ceram Soc. Bull*. **63** (1984) 803.
28. F. F. LANGE, B. I. DAVIS and D. O. RAYLEIGH, *ibid.* **66** (1983) C-50.
29. A. G. EVANS and E. A. CHARLES, *J. Amer. Ceram. Soc*. **59** (1976) 371.
30. K. NIIHARA, R. MORENA and D. P. H. HASSELMAN, *J. Mater. Sci. Lett*. **1** (1982) 13.
31. K. NIIHARA, R. MORENA and D. P. H. HASSELMAN, *J. Amer. Ceram. Soc.* **65** (1982) C-116.
32. R. M. SPRIGGS, L. A. BRISSETTE and T. VASILOS, *Mater. Res. and Stands*. **4** (1964) 218.

*Received 12 April 1999*
*and accepted 21 September 2000*